Application of concrete compression constitutive model based on energy damage

Na Xu*
College of Architectural Engineering, Guangdong Polytechnic of Science and Technology, Zhuhai 519090, Guangdong, China

ABSTRACT

In paper, according to the concrete compression damage constitutive relationship of energy loss, a cylindrical reinforced concrete shear wall with a rectangular section was simulated using ABAQUS software. The skeleton curve for structural ultimate bearing capacity was drawn under the theoretical condition, and the comparative analysis of fitting was carried out, consequently the macroscopic approximate relationship between material damage and structural failure was established, which also proved the rationality of the hypothesis. The advantages of this method are fewer parameters, simple and practical, and high precision, which can provide another solution for the simulation analysis of compressive damage of concrete structures.

Keywords: Constitutive relationship, energy loss, shear wall, skeleton curve, comparative analysis of fitting

1. INTRODUCTION

Currently, the research of damage theory has been widely used in concrete[1-6]. Using the damage force theory for analyzing concrete mechanical properties is appropriate and reasonable. It is very important to introduce the damage variables. First, according to the Najar damage theory, References[7-12] define the damage of concrete with energy loss. Then, using this kind of concrete compression damage model, we establish a new concrete compression curve damage model and evolution equation about damage. They are given that damage equations of concrete having different strengths. In paper, a rectangular shear wall model of reinforced concrete tubular is established using the constitutive model, and the skeleton curve of ultimate bearing capacity for the model structure is drawn. By fitting comparative analysis, the macroscopic approximate relationship between material damage and structural damage is established, which also proves that the model assumption is reasonable.

2. ESTABLISHMENT OF CONSTITUTIVE MODEL

The shear wall is simulated by 4-node reduced integral shell element in ABAQUS software. The shear wall section without holes is 8000×300 mm, the shear wall with opening section is 3000×300 mm, and the opening size is 900×300 mm. The storey height is 3 m. It is a ten-layer structure with full symmetrical and the bottom is consolidated. The steel reinforcement bar adopts HRB335, where f_y=335 N/mm^2, E_s=2×105 N/mm^2, ε_y=0.001675, E_s'=0.01, E_s=2×103 N/mm^2, v=0.3. The reinforcement ratio of section is 0.5%. The concrete is C35. The function curve of stress-strain relationship under non axial compression is as shown in Figure 1. The proposed plastic damage model of concrete under non axial compression is used[6], as shown in Figure 2. Without considering the tension damage of concrete the tension stress-strain relationship is simplified:

$$f_{\mathrm{t}} = \frac{1}{10} f_{\mathrm{ck}} \tag{1}$$

Under non axial compression the stress-strain relationship of concrete:

$$x \le 1 \quad y = \alpha_{\mathrm{a}} x + (3 - 2\alpha_{\mathrm{a}}) x^2 + (\alpha_{\mathrm{a}} - 2) x^3 \tag{2}$$

$$x > 1 \quad y = \frac{x}{\alpha_{\mathrm{d}}(x-1)^2 + x} \tag{3}$$

$$x = \frac{\varepsilon}{\varepsilon_o}, \quad y = \frac{\sigma}{f_c^*}$$

*174600556@qq.com

International Conference on Optics, Electronics, and Communication Engineering (OECE 2024), edited by Yang Yue, Proc. of SPIE Vol. 13395, 133952S · © 2024 SPIE · 0277-786X · Published under a Creative Commons Attribution CC-BY 3.0 License · doi: 10.1117/12.3048930

where, α_a, α_d are the parameter values of curve between stress and strain under non axial compression for the ascending and descending sections ; f_c^* is the non axial compressive strength for concrete (f_{ck}, f_c, f_{cm}); ε_c is the peak of concrete compressive strain corresponding with f_c^* .

The variable relationship of concrete damage under non axial compression:

$$0 \leq x \leq 1\ ,\quad d_c = 1 - \sqrt{\frac{\alpha_a + (3-2\alpha_a)x + (\alpha_a - 2)x^2}{\alpha_a}} \tag{4}$$

$$x > 1, d_c = 1 - \left[\frac{1}{\alpha_a[\alpha_d(x-1)^2 + x]}\right]^{\frac{1}{2}} \tag{5}$$

$$\varepsilon_o = (700 + 172\sqrt{f_c^*}) \times 10^{-6}, \alpha_a = 2.4 - 0.0125 f_c^*, \alpha_d = 0.157 f_c^{*0.785} - 0.905, f_c^* = f_{ck} = 0.7R.$$

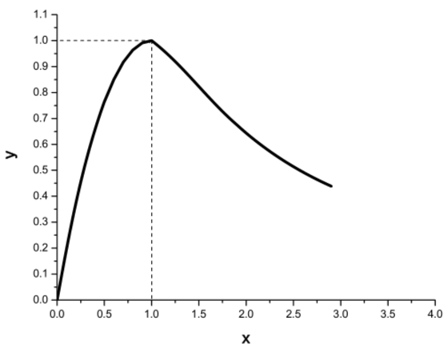

Figure 1. The relation of concrete compression between stress and strain.

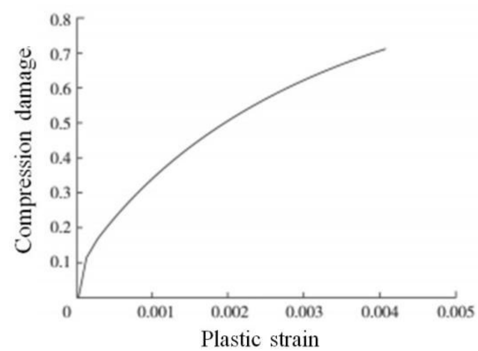

Figure 2. The relationship curve between compression damage variable and plastic strain (C35).

3. ELASTIC ANALYSIS

First, the stress, vertical displacement and vertical reaction at the bottom section of the structure were examined respectively in the elastic range under the action of self-weight, and the model was verified to be reasonable and effective. Selecting a section on the wall with hole at the bottom of the structure, and the stress values of nodes 1 to 7 on this section are 0.760, 0.717, 0.675, 0.674, 0.674, 0.716, 0.759 N/mm^2, respectively. The stress distribution for the section is shown in Figure 3. From Figure 3, at the end of section stress concentration occurs, with continuous diffusion of stress to the middle section, the stress gradually reaches a uniform distribution in the middle position, and for the symmetric nodes stress is basically same, and stress value for each section is almost same.

The vertical reaction values of the seven nodes of this section are 62.7, 110.5, 106.4, 104.6, 106.2, 110.0 and 62.6 kN respectively (Figure 4). Axial reaction is generated at the bottom node, and the stress concentration occurs at the corner. Here the vertical reaction is small, the vertical reaction of the middle section is large, and the joint reaction for symmetrical section is almost same. The vertical displacement values of 7 nodes in this section are all 0.34 mm, which indicates that the numerical simulation conforms to the theory, so we can get that model is reasonably available.

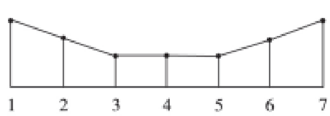

Figure 3. Stress distribution of bottom cross-section.

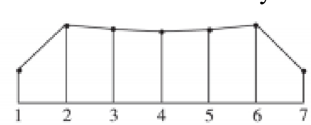

Figure 4. Reaction force distribution.

4. ELASTOPLASTIC ANALYSIS

This model is applied to the elastoplastic analysis. The different combinations are selected and the horizontal loads and vertical loads on the model are applied at the same time, that is, the horizontal loads are input but the axial forces remain unchanged. The axial pressure and bending moment of the biased member are interrelated when the member is in the limit state of normal section bearing capacity. Using software Matlab the program of N_u-M_u curve is drawn according to the following steps, in order to obtain the skeleton curve of N_u-M_u theory for the ultimate bearing capacity of the structure under bias pressure:

(1) The compressive strain at the compressive edge of concrete is selected as ε_{cu};

(2) Selecting the edge strain of the tension side;

(3) According to the non axial tensile and compressive constitutive model for concrete, the non axial tensile and compressive constitutive model for steel bar and the strain distribution of cross-section, not only concrete stress but also tensile and compressive stress for steel bar are obtained;

(4) The pressure N_u and bending moment M_u are calculated according to the equilibrium condition;

(5) Selecting another edge strain on the tension side, as shown in Figure 5, and repeat steps (3) and (4).

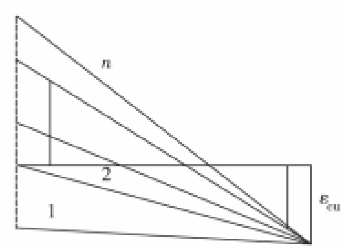

Figure 5. Computing model.

In the actual situation, when the vertical load is applied, the member is in a state of full section compression, due to stress concentration and other reasons, the cross sections of the left and right ends will appear false damage. So, we do not consider the false damage in the end section, and only study the middle section. The results show that the damage variable values of the whole section reach the critical value of damage, and the whole section is destroyed. When the horizontal load and vertical load are applied to the model at the same time, the right section enters the damage state first. With the increase of load, the damage expands, and the left section begins to be damaged gradually. In the study of all combinations under the action of bias pressure, the critical value of damage first appears at the compression edge of the section.

It is assumed that when 7% of the compression section reaches the critical value of damage, the structure is defined as failure. At this time, it is the ultimate bearing state, and the internal force SF_i is obtained. After processing the internal force SF_i data, the N_u-M_u combination is obtained,

where

$$N_u = \sum_{i=2}^{16} SF_i \tag{6}$$

Assuming that the pressure is in a positive direction, SF_i takes a moment to the middle point

$$\begin{aligned} Mu = {} & SF_2 \times a_2 + SF_3 \times a_3 + SF_4 \times a_4 + SF_5 \times a_5 + SF_6 \times a_6 + SF_7 \times a_7 + SF_8 \times a_8 + SF_9 \times a_9 + \\ & SF_{10} \times a_{10} + SF_{11} \times a_{11} + SF_{12} \times a_{12} + SF_{13} \times a_{13} + SF_{14} \times a_{14} + SF_{15} \times a_{15} + SF_{16} \times a_{16} \end{aligned} \tag{7}$$

where

a_2=3.5, a_3=3.0, a_4=2.5, a_5=2.0, a_6=1.5, a_7=1.0, a_8=0.5, a_9=0, a_{10}=0.5, a_{11}=1.0, a_{12}=1.5, a_{13} =2.0, a_{14}=2.5, a_{15}=3.0, a_{16}=3.5

By using equation (7), the total structural axial force N_u and total bending moment M_u under actual bias can be obtained. By applying the existing program of drawing Nu-Mu skeleton curve, the theoretical skeleton curve of ultimate bearing capacity can be obtained. Between the total axial force N_u and total bending moment M_u the theoretical skeleton curve were obtained through comparative study and analysis. It is shown in Figure 6. All failure cases of the structure under eccentric compression are included in the ultimate bearing capacity skeleton curve, in which the tensile failure of concrete is the stage when the axial force is negative. We only study the actual compression failure, including large and small bias:

(1) When the bending moment is 0, the axial force reaches the limit value;

(2) When axial force is 0, bending moment does not reach the breaking point. The bending moment reaches the breaking point when the boundary failure occurs;

(3) In the stage of small bias pressure, the axial force decreases with the increase of bending moment; In the stage of large bias pressure, the axial force increases as the bending moment increases.

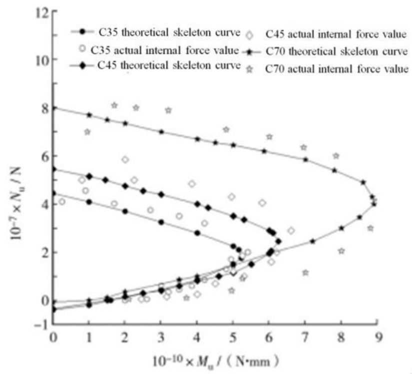

Figure 6. Simulation and comparison of N_u-M_u.

The structural failure is all under this damage degree, and the internal force combination conforms to the theoretical curve. It indicates that the macroscopic failure assumption of the whole section is reasonable.

The results show that no matter what the strength level of concrete is, when the compression damage value of 7% of the structure is close to or beyond the critical value of the compression damage, the structure reaches the limit state and the failure occurs.

Being different from previous studies, it mainly relies on the microscopic properties of materials to determine whether the structure is damaged, this study establishes a macroscopic relationship between damage and damage based on the theoretical skeleton curve when the compression damage value of 7% of the section of the member approaches or exceeds the critical value of the compression damage, the member reaches the limit state and the failure occurs.

5. CONCLUSION

By using this mathematical model, the nature and variation rules of non axial compression damage of concrete are revealed, and the data and reference of the damage mechanism for concrete structure are provided. The constitutive model has many advantages, such as few parameters, very simple formula, practical method, high precision. It reveals the macroscopic relationship between the material damage degree and the structural damage in the actual situation.

REFERENCES

[1] Yang, W., [Research on Theory and Experiment of Concrete Elastoplastic Damage Constitutive Relation], Shanghai: Tongji University, Master's Thesis, (2007).

[2] He, J., Ma, H. and Chen, H., "Summarize on the concrete damage constitutive theory research," Advances in Science and Technology of Water Resources 30(3), 89-94 (2010).

[3] Qi, H., Li, Y. and Lv, X., "A practical elastic plastic damage constitutive model based on energy," Engineering Mechanics 30(5), 172-180 (2013).

[4] Jordan, S. P., Kawachi, I. I. and Subramanian, S. V. S. V., "Compelling care: A grounded theory of transmasculine self-defense and collective protection at the clinic," Social Science & Medicine, 345, 1-8 (2024).

[5] Dongmo, B., "A 3D visco-elasto-plasto damage constitutive model of concrete under long-term effects, "Materials Research Forum LLC, 26, 35-40 (2023).

[6] Soysal, B. F., Arici, Y. and Tuncay, K., "A modified applied element model for the simulation of plain concrete behaviour," Magazine of Concrete Research, 75(7), 325-338 (2022).

[7] Al-Saffar, F. Y., Wong, L. S. and Paul, S., "An elucidative review of the nanomaterial effect on the durability and calcium-silicate-hydrate (C-S-H) gel development of concrete," Creative Commons Attribution, 613(9), 1-37 (2023).
[8] Castorrini, A., Ortolani, A. and Campobasso, M. S., "Assessing the progression of wind turbine energy yield losses due to blade erosion by resolving damage geometries from lab tests and field observations," Renewable Energy at International Journal, 218, 1-13 (2023).
[9] Bar, A. K., Basu, A., Barman, S. and Banik, R., "A study of the average energy loss to the acoustic modes and the non-ohmic mobility characteristics of a degenerate semiconductor using an alternative model of heated Fermi-Dirac distribution," 4th International Conference on Current Trends in Materials Science and Engineering 2022, 1-14 (2024).
[10] Xu, N., [Damage Determine and Identification of Reinforced Concrete Structure], Harbin Institute of Technology, Harbin, (2008).
[11] Xu, N., Fu, X., "The compression damage constitutive model of concrete based on the theory of energy loss," Journal of Shenzhen University Science and Engineering 6, 604-610 (2017).
[12] Xu, N., "A new compressive damage constitutive model for concrete," Advances in Transdisciplinary Engineering 31, 420-426 (2022).